Shock Tube Performance Studies With Air And Carbon Di-Oxide Using Numerical Simulation

Arjun Jayakumar , Arun Danam , Asok Kumar N
College of Engineering Trivandrum
Department of Mechanical Engineering
arundanam@gmail.com, arjunjk91@gmail.com, asoknak@cet.ac.in

***Abstract*— This paper investigates the performance of a shock tube with air and carbon dioxide as working fluids at different diaphragm pressure ratios using numerical simulations. A Parametric study was also carried out to find the effects of diaphragm pressure ratios on the shock Mach number and the temperatures behind the incident and reflected shock waves. Dependency of shock Mach number, temperature and pressure behind incident and reflected shock on diaphragm pressure ratio are obtained. Shock Mach number, pressure and temperature of shocked gas, obtained at different diaphragm pressure ratios were compared to bring out the relative advantages and disadvantages of using carbon dioxide compared to air. By increasing the diaphragm pressure ratio, higher shock Mach numbers can be obtained with carbon dioxide compared with air as working fluid inside the shock tube. However, carbon dioxide gives lower temperature behind incident and reflected shock waves compared with air.**

Keywords—shock tube , pressure ratio, reflected wave

I. INTRODUCTION

Shock tube based research has over the last five decades uncovered several potential areas for scientific investigation. The main thrust was focused on applying the shock tube for aerodynamic and high temperature chemical kinetic studies with test times of less than 1ms. It is also used to replicate and direct blast waves at a sensor or a model in order to simulate actual explosions and their effects, usually on a smaller scale. Shock tube in its simplest form consists of a uniform cross-section tube divided into driver and driven sections by a diaphragm. The driver section is filled with a high pressure gas and driven section contains the gas at low pressure. The driver section is pressurized high enough to cause the diaphragm to rupture and as a result, a shock wave is generated and travels down the driven tube. Simultaneously, an expansion fan propagates through the high-pressure side.

Figure 1 shows flow fields in an idealized shock tube. The low-pressure side (state-1) is shown on the right of the diaphragm, this is the experimental gas which is subjected to the shock wave. The high-pressure side, containing driver gas (state-4), is shown on the left. At time "t = 0" the diaphragm is assumed to rupture instantaneously. After the bursting of diaphragm, compression waves are formed in the low-pressure gas, this rapidly steepening to form a shock front, state-2 behind the shock will show an abrupt rise in temperature and pressure. Simultaneously, an expansion or rarefaction wave moves back into the high pressure region. The front of this rarefaction travels back with the speed of sound in the driver gas, but the pressure fall is smooth, not discontinuous as in the shock front. This rarefaction wave is often referred to as an "expansion fan" and the gas behind expansion wave is designated as state-3 having lower pressure and temperature. The experimental gas and the driver gas make contact at the 'contact surface', which moves rapidly along the tube behind the shock front. Both shock and rarefaction waves reflect as they reach the endwall of the shock tube and a change in state of gas behind the waves to state 5 and 6 respectively.

The movements of the contact surface and the rarefaction wave are shown in the (x-t) diagram in Figure 1. In ideal case the temperature shows an abrupt rise from initial room temperature to a very high value at the shock front, remains steady up to contact surface, where it falls quickly to a value well below room temperature. And then in the rarefaction fan rises slowly again to the initial temperature.

Most of the earlier studies modeled shock tube flow as one dimensional, which fail to simulate highly nonlinear physical process whereas multi-dimensional simulations can accurately model the unsteady flow. Argow, B. M [1] and Sheng, Y [2] have proposed a 1-D technique for shock tube and shock tunnel flow simulation. Hatem Ksibi and Ali Ben Moussa [3] have numerically simulated one dimensional shock tube flow for supercritical fluid. Sod problem [4] is an essentially one-dimensional flow discontinuity problem which provides a good test of a compressible code's ability to capture shocks

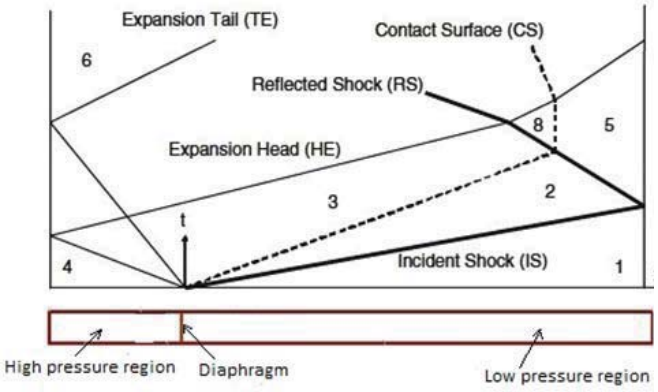

Fig. 1. Ideal shock tube flow.

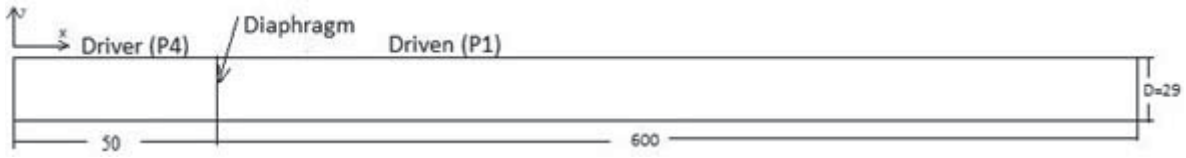

Fig. 2. Schematic diagram of computational domain.

and contact discontinuities with a small number of zones and to produce the correct density profile in a rarefaction. Mouna Lamnaouer, [5] have done extensive studies on numerical simulation of shock tube with variable area of cross section. Chang and Kim [6] developed a two dimensional inviscid numerical simulation in expansion tube with the FCT (Flux-Corrected Transport) discretization scheme.

The studies mentioned above have given insight into the flow evolution in shock tubes and the various non-ideal phenomena that affect the test time. Arjun Jayakumar [7] have numerically modeled the flow inside the shock tube under consideration and validated it theoretically using the Rankine–Hugoniot normal shock relation. The model considered air as driver and driven gas, the same model is used to conduct parametric analysis using carbon di-oxide gas and the performance of shock tube will be compared with air as working fluid. One particular benefit of this study is the development of a fluid mechanics model of the reflected shock process that can be applied to future experimental works.

A time accurate two dimensional inviscid shock tube model has been developed to conduct parametric study and this model will simulate the propagation and reflection of shock wave. Parametric studies were conducted for air and carbon dioxide gases at both driver and driven sections. Numerical simulations were carried out in CFD solver ANSYS Fluent 14. Adaptive mesh refinement (AMR) technique was applied to the time-dependent flow fields to accurately capture and resolve the shock and contact discontinuities. This study accurately predict the diaphragm pressure ratios required for desired level of shock Mach number and temperature behind incident and reflected shock wave. The shock wave motion, reflection and interaction with end walls were investigated and their influence on the performance of the shock tube was determined. Complete flow simulation of shock tube will provide valuable information on interaction of contact surface with expansion fan and shock wave will determine the maximum test time.

I. NUMERICAL MODELLING

A. Governing Equation

The flow is assumed to be inviscid for modelling the complex mechanisms responsible for the non-uniform conditions and the reduced test times in the shock tube. Considering a non viscous flow in a tube, Navier–Stokes equations reduce to Euler equations. Euler equation is basically a non-linear hyperbolic partial differential equation. The conservative form of Euler equation in Cartesian coordinate two dimension is given by "(1)"

$$\frac{\partial U}{\partial t}+\frac{\partial E}{\partial x}+\frac{\partial F}{\partial y}=0 \tag{1}$$

Where vectors U, E and F are defined as

$$U=\begin{bmatrix}\rho\\ \rho u\\ \rho v\\ \varepsilon\end{bmatrix};E=\begin{bmatrix}\rho u\\ \rho u^2+p\\ \rho uv\\ u(\varepsilon+p)\end{bmatrix};F=\begin{bmatrix}\rho v\\ \rho uv\\ \rho v^2+p\\ v(\varepsilon+p)\end{bmatrix} \tag{2}$$

Specific Energy is given by

$$\varepsilon=\frac{1}{\gamma-1}\frac{p}{\rho}+\frac{1}{2}\left(u^2+v^2\right) \tag{3}$$

Pressure

$$p=(\gamma-1)\left(\varepsilon-\frac{1}{2}\rho\left(u^2+v^2\right)\right) \tag{4}$$

Where, U represents the conserved variables E and F are the overall fluxes in x,y-directions respectively, ρ, u and v the density and velocity per unit mass of the fluid in x and y direction respectively.

B. Flow Domain

Entire geometry of the high-pressure shock tube is modeled. The shock tube consists of a 50mm long driver section and a 600 mm long driven section with a uniform internal diameter of 29 mm. Two dimensional approach to the cylindrical geometry of the shock tube gives a rectangular flow domain (650mm x 29mm) sufficient to render an accurate description of the real flow configuration. Figure 2 shows the schematic diagram of the shock tube under consideration. Complete area inside the shock tube is considered for the computation since the entire flow has to be simulated.

C. Meshing

Meshing of the flow domain is done by uniform quadrilateral method. Mesh independency study conducted gives mesh saturation at 20000 nodes. Accurate solutions can

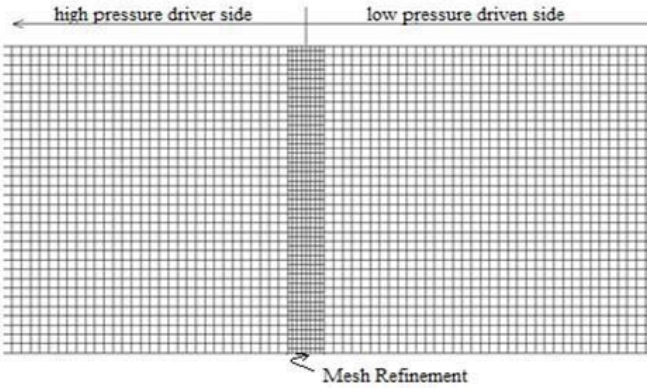

Fig. 3. Initial grid around diaphragm section

TABLE I. Initial conditions for which simulations were done

P_1 (atm)	Air		Carbon dioxide	
	ρ_4 (kg/m^3)	ρ_1 (kg/m^3)	ρ_4 (kg/m^3)	ρ_1 (kg/m^3)
1	7.013	1.169	10.65	1.7761
0.8	7.013	0.9351	10.65	1.42
0.6	7.013	0.7013	10.65	1.065
0.4	7.013	0.4676	10.65	0.71
0.3	7.013	0.3507	10.65	0.5328
0.21	7.013	0.2445	10.65	0.3729

be obtained with structured mesh in which grid lines are aligned in the flow direction. A grid adaptation tool Adaptive Mesh Refinement (AMR) is used to resolve regions with the steepest gradients. AMR technique was effectively used to create cluster of cells around density gradient region. Figure 3 shows the initial grid around the diaphragm where, density gradient exist. Additional cells are added in the flow domain as necessary via grid adaptation to maintain finer mesh around the shock and contact discontinuities and thus reduce the error in solution. As such, the computational efforts are focused around high gradient flow fields all by keeping the overall computational time to a minimum. As the shock propagates, the position of density gradient changes and this will result in a dynamic mesh adaptation. The adaptive grid refinement has been successfully used to resolve regions with the steepest gradients. The solution is independent of the mesh size and adequate resolutions of flow field have been achieved.

D. Initial and boundary conditions

Shock tube has closed ends at both right and left boundaries of the computational domain. Solid wall boundary condition is assumed, so for the momentum equations no mass fluxes can penetrate through the solid boundary. Before performing iterations, initial flow field variables must be specified at all points in the domain. The initial solution of the problem consists of two uniform states, separated by a discontinuity 50mm from left end wall. Pressure values are specified at both the driver and driven sections, in accordance with the desired pressure ratio. Simulations were carried out for different initial conditions. Before rupture, gases are in stagnant condition and also uniform temperature of 302 K is assumed at both driver and driven gas for all simulations. For all simulations driver side pressure is fixed to 6 atm. Since the flow is assumed inviscid no adhesion of fluid layer over the wall surface and hence slip boundary condition is imposed. For the energy equation, adiabatic wall condition is applied.

E. Numerical Scheme

Control volume approach and density-based explicit solver is used for discretizing model equations are in space and time. The flow domain is represented with a structured mesh of quadrilateral cells. Flux vectors are computed with AUSM+ flux vector splitting scheme which is suitable for capturing shock waves. The convective terms are discretized in space following second order upwind scheme which provide an

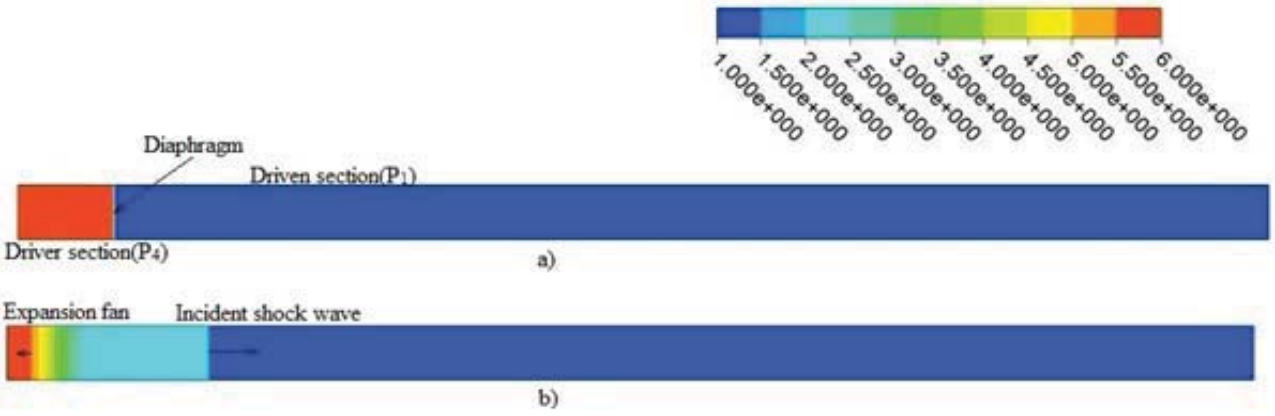

Fig. 4. Contours of pressure (in atm) a) initial b) after 110μs of diaphragm rupture

Fig. 5. Contours of temperature (in K) after 110μs of diaphragm rupture

Fig 6. Shock wave reflection from end wall creating high temperature behind shock

accurate and stable solution. An explicit time-stepping integration was performed using a four-stage Runge-Kutta scheme for unsteady flows. The time step was set by the Courant-Friedrichs-Lewy stability limit between 0.4 and 0.8.The density-based coupled-explicit algorithm is adopted with single precision. This algorithm solves the governing equations of continuity, momentum and energy simultaneously as a set of equations.

II. RESULT AND DISCUSSION

Extensive CFD analyses were carried out for different pressure ratios ranging from of 6 to 28 with air and carbon dioxide as working gases. Parametric analysis is done by comparing the flow properties behind incident and reflected shock for both gases. Effect of initial pressure ratio across the diaphragm on the shock Mach number, incident shocked gas temperature and reflected shocked gas temperature are studied.

Figure 4 (a) shows the pressure distribution across the shock tube before diaphragm rupture with a pressure ratio of 6 with air as working gas. Pressure contours can resolve incident and expansion fan as shown in figure 4 (b). Contact surface which is formed at the interface of two gas cannot be differentiated in pressure profile as no pressure gradient exist across the surface but temperature contours can differentiate all the three discontinuities. Pressure and temperature behind incident shock wave rise to 2.5 atm and 391K respectively as shown in figure 4 (b) and 5. Incident shock wave moving towards right side will reflect from end wall and raises the temperature behind the shock to 480K as shown in figure 6. Also, from the full simulation of shock tube flow it is evident that driver gas contamination does not occur until shock wave is being reflected from end wall and sufficient test time is available.

Figure 7 shows the diaphragm pressure ratio required for generating the required Mach number with air and carbon dioxide. At lower pressure ratios both gases generate almost equal shock Mach numbers. As pressure ratio increases above 10 considerable deviation occurs in the generated shock Mach number. By using carbon dioxide instead of air, 2% hike in Mach number is noted at a pressure ratio of 28.This shows that significant rise in Mach number and hence high shock strength can be achieved with carbon dioxide at higher pressure ratios. One of the major applications of shock tube is in the field of ballistic studies. The flow field of a ballistic wave can be approximated as a lead shock wave. High explosives, which detonate, generate blast waves. Ballistic studies deal with these types of shock waves, it is evident from the studies that carbon dioxide is preferable compared to air for conducting ballistic experiments which require shock of higher strength.

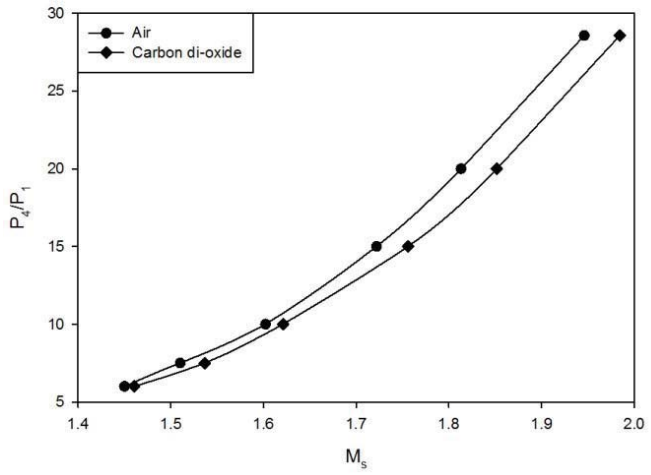

Fig. 7. Diaphragm pressure ratios required to generate incident shock Mach numbers

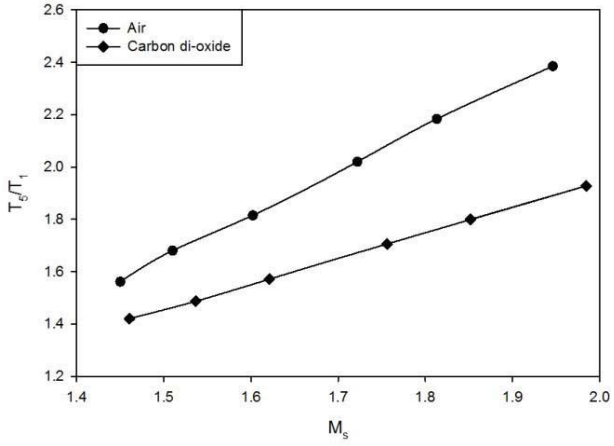

Fig. 9. Dimensionless reflected gas temperature to shock Mach number

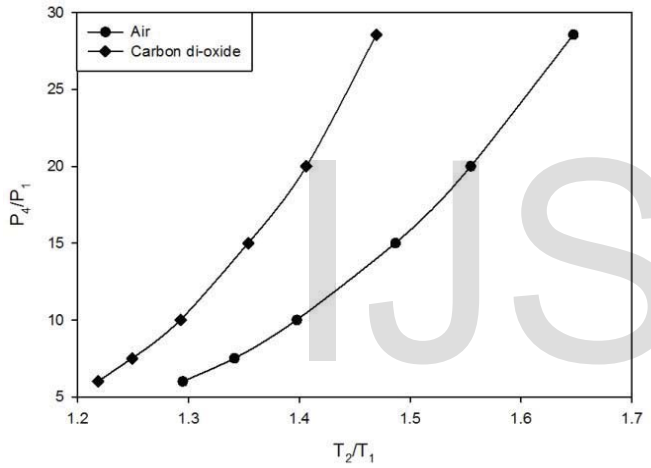

Fig. 8. Dependency of diaphragm pressure ratio on temperature of shocked gas

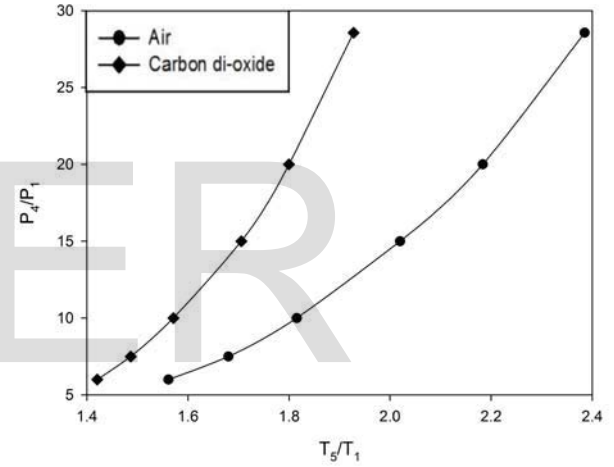

Fig. 10. Diaphragm pressure ratio to non dimensional temperature behind reflected shock

Figure 8 compares the effect of diaphragm pressure ratio on temperature behind the incident shock wave (T_2) with carbon dioxide and air as working fluids. As the diaphragm pressure ratio increases, as expected, the temperature behind the shock wave increases for both the working fluids. However, the temperature (T_2) in the case of carbon dioxide is less compared to air for a particular diaphragm pressure ratio. When the pressure ratio increases from 6 to 28, the increase in temperature behind the shock wave is found to be75K for carbon dioxide and 108 K for air. The hike in T_2 for air compared with carbon dioxide changes from 21 K to 54 K as the pressure ratio changes from 6 to 28 showing that the effect is going to be significant at still higher pressure ratios. Temperature behind incident shock is a function of specific. heat ratio and shock Mach number. As evident from figure 8 air has higher temperature behind the incident shock wave which favors chemical kinetics study at higher temperature.

Figure 9 compares the effect of shock Mach number on temperature behind the reflected shock wave (T_5) with carbon dioxide and air as working fluids. As the shock Mach number increases, as expected, the temperature behind the reflected shock wave increases for both the working fluids. However, the temperature (T_5) in the case of carbon dioxide is less compared to air for a particular shock Mach number. When the shock Mach number increases from 1.5 to 1.9, the increase in temperature behind the shock wave is found to be 150K for carbon dioxide and 240 K for air. The hike in T_5 for air compared with carbon dioxide changes from 54 K to 150 K as the shock Mach number changes from 1.5 to 1.9 showing that

the effect is going to be significant at still higher shock Mach numbers.

Figure 10 shows the diaphragm pressure ratio required for generating the required temperature behind the reflected shock wave (T_5) with air and carbon dioxide as working fluids. As the diaphragm pressure ratio increases, as expected, the temperature behind the reflected shock wave increases for both the working fluids. However, the temperature (T_5) in the case of carbon dioxide is less compared to air for a particular diaphragm pressure ratio. When the pressure ratio increases from 6 to 28, the increase in temperature behind the reflected shock wave is found to be 150K for carbon dioxide and 250 K for air. The hike in T_5 for air compared with carbon dioxide changes from 42 K to 140 K as the pressure ratio changes from 6 to 28 showing that the effect is going to be significant at still higher pressure ratios.

III. Conclusion

Parametric shock tube studies are conducted for different pressure ratios and its effects on the temperature ratio and Mach number are discussed for air and carbon dioxide as working fluids. It is observed that incident shock is followed by contact surface up to the endwall with both gases so that experiments can be conducted in incident and reflected mode. Dependency of shock Mach number, temperature and pressure behind incident and reflected shock on diaphragm pressure ratio are obtained. By increasing the diaphragm pressure ratio, higher shock Mach numbers can be obtained with carbon dioxide compared with air as working fluid inside the shock tube. However, carbon dioxide gives lower temperature behind incident and reflected shock waves compared with air. From the parametric studies conducted it can be concluded that air gives superior test conditions for kinetics studies whereas carbon dioxide has slight upper hand for ballistic studies.

References

[1] Argow, B. M., “Computational analysis of dense gas shock tube flow”, ShockWaves, Vol. 6, pp. 241-248. 1996

[2] Sheng, Y., Sislian, J. P., and Liu, J. J., “A computational technique for high enthalpy shock tube and shock tunnel flow simulation” , Shock Waves, Vol. 8, pp. 203-214. 1998

[3] HatemKsibi and Ali Ben Moussa, “Numerical simulation of a one-dimensional shock tube problem at supercritical fluid conditions” , International Journal of Physical Sciences, Vol. 3 (12), pp. 314-320. 2007

[4] Gary A Sod , “A survey of several finite difference methods for systems of nonlinear hyperbolic conservation laws”, Journal of computational physics, Vol 27, pp.1-31. 1978

[5] Mouna Lamnaouer, “Numerical modelling of the shock tube flow fields before and during ignition delay time experiments at practical conditions” , Ph.D. Thesis 2004

[6] Chang, K. S. and Kim, J. K., “Numerical investigation of inviscid shock wave dynamics in an expansion tube” , Shock Waves, Vol. 5, pp. 33-45. 1995

[7] Arjun Jayakumar, “Numerical modelling and theoretical validation of shock tube flow” , International Journal of Applied Engineering Research, ISSN 0973-4562 9(5),537-544. (2014)